Journal of Statistical Physics, Vol. 82, Nos. 5/6, 1996

Anisotropic Finite-Size Scaling Analysis of a Two-Dimensional Driven Diffusive System

Jian-Sheng Wang[1]

Received December 13, 1994; final August 4, 1995

The standard two-dimensional uniformly driven diffusive model is simulated extensively for much larger systems with a multi-spin coding technique. The nonequilibrium phase transition is analyzed with anisotropic finite-size scaling both at the critical point and off the critical point. The field-theoretic values of critical exponents fit the data well at and above T_c. Below T_c the scaling is rather difficult and the results are not conclusive.

KEY WORDS: Driven diffusive systems; anisotropic finite-size scaling; nonequilibrium phase transitions; computer simulations.

1. INTRODUCTION

Driven diffusive systems are a class of models which exhibit nonequilibrium phase transitions,[1-4] (see refs. 4 for reviews). The models are defined by some local rules which do not satisfy detailed balance. The steady states of the dynamical evolution have been studied extensively during the past decade. A central issue is the extent to which the concept of universality of critical phenomena can be applied in nonequilibrium cases.

The standard driven diffusive model of half-filled charged lattice gas was proposed as a model for an ionic solution in an electric field.[1, 2] A continuum version, based on symmetries and conservation laws, was solved in a field-theoretic framework.[5, 6] It is quite remarkable that exact critical exponents are obtained for dimensions from two to five. In particular, the set of critical exponents in two dimensions is

$$\beta = 1/2, \qquad \gamma = 1, \qquad \nu_{\parallel} = 3/2, \qquad \nu_{\perp} = 1/2 \tag{1}$$

[1] Computational Science, National University of Singapore, Singapore 119260. E-mail: cscwjs@leonis.nus.sg.

822/82/5-6-13

These exponents have a similar meaning as in equilibrium second-order phase transitions. They are thought to be universal within the class. Note that $\nu_{\|} \neq \nu_{\perp}$. This implies an intrinsic anisotropy in the system which cannot be scaled away.

Computer simulations[7-11] have been applied to the problem to check the validity of the results. Anisotropic finite-size scaling studies by Leung[8,9] appear to have settled a dispute between theory and early computer simulations. But recent work by Achahbar *et al.*[10,11] casts doubt on Leung's conclusion. We made an extensive simulation study of the model, and the results are largely consistent with Leung's findings. The high-precision data presented here support the anisotropic finite-size scaling theory with the set of exponents (1) at and above T_c. However, the interpretation of the data below T_c is difficult.

2. MODEL AND SIMULATION

Our system consists of a square lattice of $L \times M$ sites. The driven field is in the x direction. A configuration is a set of Ising spins, $\sigma_{x,y} = \pm 1$, located at each site, with zero total magnetization. Equivalently, the system can also be viewed as a half-filled lattice gas, with $\sigma_{x,y} = 1$ corresponding to an occupied site and -1 an empty site. The state evolves according to the following prescription. A bond is chosen with equal probability in orientations and in locations. If the bond is parallel to the driven field and the adjoining spins are distinct, the spins are set to $\sigma_{x,y} = -1$ and $\sigma_{x+1 \bmod L, y} = +1$. This corresponds to an infinitely strong driven field. If the bond is perpendicular to the field, we swap the spin values with the Metropolis probability $\min\{1, \exp(-\delta E/k_B T)\}$, where δE is the energy increment due to the change, assuming the usual nearest neighbour ferromagnetic interaction with coupling constant J and periodic boundary conditions. One Monte Carlo step is defined as $L \times M$ such basic steps.

Simulation near the critical point is notoriously difficult because of critical slowing down. The situation for this model is more severe due to the conservative nature of the dynamics, leading to relaxation time $\tau \propto M^4$. Thus, an efficient implementation is crucial to obtaining good statistics. We used a multi-spin coding method,[12,13] by which 32 systems are simulated simultaneously on 32-bit computers. This appears to be the method of choice without changing the definition of the model. It gives us at least a factor of 20 speedup over a straightforward program. A slight penalty of the multi-spin coding algorithm is that the temperature cannot be set exactly to a given value. But it can be well under control with a large random bit table. To achieve an accuracy of five significant figures in temperature, we took a random bit table of 2^{18} entries.

The program runs at 0.3 μ sec per spin exchange on an SGI Indigo Workstation. Computations were done on a cluster of fifty workstations (SGI Indigo, HP 9000/700 model 712, and DEC 5000) over several months. The lengths of the runs are mostly 10^7–10^8 Monte Carlo steps. These are orders of magnitude longer than in previous studies. The systems are started from a completely ordered state (a strip along the x direction), and a large number of Monte Carlo steps is discarded for equilibration. Over 70 different systems are simulated, from system size 4×4 to 1024×128. Measurements are performed at an interval of 10 Monte Carlo steps. We use the order parameter introduced by Wang *et al.*[14] and modified by Leung.[8] Let us define

$$\phi=\frac{1}{2L}\sin\left(\frac{\pi}{M}\right)\left|\sum_{x=0}^{L-1}\sum_{y=0}^{M-1}\sigma_{x,y}e^{i2\pi y/M}\right| \tag{2}$$

The normalization is such that $\phi=1$ for a strip geometry (the configuration in the limit $T\to0$). The following quantities are calculated: (a) the order parameter $\Psi=\langle\phi\rangle$, (b) the "susceptibility," or fluctuation of the order parameter,

$$\chi=\frac{L}{\sin(\pi/M)}[\langle\phi^2\rangle-\langle\phi\rangle^2] \tag{3}$$

and the "susceptibility" above the critical temperature,

$$\chi'=\frac{L}{\sin(\pi/M)}\langle\phi^2\rangle \tag{4}$$

and (c) the fourth-order cumulant,

$$g=2-\frac{\langle\phi^4\rangle}{\langle\phi^2\rangle^2} \tag{5}$$

Note that g goes from 0 to 1 as temperature T goes from ∞ to 0. We measure temperature in units of the two-dimensional Ising critical temperature ($2.269J/k_B$).

Local quantities like pair-correlation functions are rather difficult to analyze. In addition, much more data need to be handled. We prefer to work on a small data set (Ψ, χ, g) for each temperature.

3. DETERMINATION OF THE CRITICAL TEMPERATURE

Estimating the critical exponents depends crucially on an accurate value of the critical temperature. In the literature different authors have

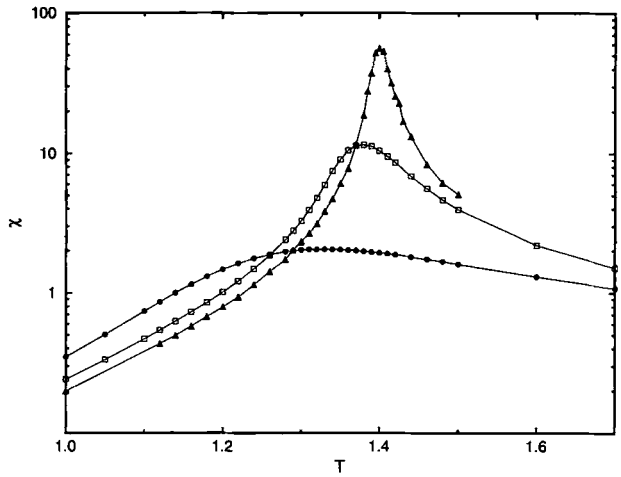

Fig. 1. The susceptibility χ vs. temperture T, for system sizes [Monte Carlo steps] of 16×16 [4×10^8] (circles), 128×32 [5×10^8] (squares), and 1024×64 [2.7×10^7] (triangles).

given incompatible values: $T_c = 1.355 \pm 0.003$ (Vallés and Marro[7]), $T_c \approx 1.38$ (Achahbar *et al.*,[11]) and $T_c = 1.418 \pm 0.005$ (Leung[8]). The discrepancies are the manifestation of the difficulties of simulating the system and of interpreting the complicated finite-size data.

Ideally, T_c should be determined independent of the assumption of critical exponents. This is not always possible. The methods used in this section are fairly standard and robust. First, we look at the peak of the susceptibility χ. Figure 1 is a typical plot for χ for a set of systems with

Table 1. Locations of the Peaks $T_c(L, M)$ in the Susceptibilities of Various System Sizes

$L\backslash M$	4	8	16	32	64	128	256
4	1.20	1.5	1.30	1.11			
8	0.79	1.29	1.31	1.21	1.1	1.05	
16		1.19	1.333	1.30	1.23	1.18	
32		1.1	1.34	1.347	1.31	1.26	
64		1.05	1.325	1.365	1.36	1.33	
128			1.31	1.380	1.38	1.374	
256			1.29	1.385	1.395	1.39	1.37
512			1.267	1.379	1.399	1.397	
1024				1.374	1.400	1.40	
2048					1.400		

fixed $S = L^{1/3}/M$. The accuracy of the peak locations depends on the accuracy of the susceptibility data and the spacing of the data points. In this calculation, the largest relative errors in susceptibility are about 10% and the spacings in T are 0.01 or 0.005. The locations of the peaks are robust, even though the susceptibility data have larger errors. The peak locations $T_c(L, M)$ are obtained by fitting the data near the peak to a parabola. Table I lists the values for a variety of geometries simulated.

The general picture of the finite-size critical temperature $T_c(L, M)$ is as follows. For very elongated shapes (when $L \to \infty$ keeping M fixed or vice versa), $T_c(L, M)$ decreases toward zero, since the systems in this limit are quasi-one-dimensional. For a fixed value M, $T_c(L, M)$ reaches its maximum at about $S = L^{1/3}/M \approx 0.2$, which we interpret as indicating that the systems with $S \approx 0.2$ notice the finiteness of the sizes in two directions at roughly the same temperature. When L is fixed, the maxima do not coincide with the former, and appear at about $L^{1/2}/M \approx 0.25$. We do not understand the reason for this discrepancy. In any case, the data indicate a large anisotropy in the system. $T_c(L, M)$ increases as system size increases with fixed S.

It appears reasonable to assume that the limit value T_c is approached from below. Then, each of the finite system values should be a lower bound for T_c. That is, we expect $T_c > 1.40$. Thus, an estimate like $T_c \approx 1.355$ or 1.38 is too low, and is due to the small system sizes used.

If the system is intrinsically anisotropic, in the sense $\nu_{\|} \neq \nu_{\perp}$, scaling functions cannot be expressed in terms of a single scaling variable. A shape factor $S = L^{\nu_\perp/\nu_\|}/M$ enters in addition to the usual scaling variable $L^{1/\nu_\|}(T - T_c)/T_c$. There is an excellent example of this behaviour of a model with an exact solution.[15] Thus, shape as well as size are important in anisotropic systems. This point is also raised by Leung and Zia, who criticized analysis based on a square geometry.[16] Binder and Wang elaborated on phenomenological anisotropic finite-size scaling theories.[17] Following these ideas, the anisotropic system has a one-variable scaling form like the isotropic one if we fix the ratio S.

We analyzed the data according to the anisotropic finite-size scaling assumption,

$$T_c(L, M) = T_c + F(S)\, L^{-1/\nu_\|} \tag{6}$$

Figure 2 is a plot of the peak locations $T_c(L, M)$ versus $L^{-2/3}$ for $S \approx 0.0625$, 0.0787, 0.157, and 0.198. The data follow this equation reasonably well.

In Fig. 3 we plot the extrapolated T_c as a function of the ratio S. The T_c values based on the assumption $\nu_\perp = \nu_\| = 1$ are also plotted. In this case, we see that the extrapolated values for T_c increase as the aspect ratio L/M increases. This general feature is insensitive to the value, of $\nu_\perp$ used.

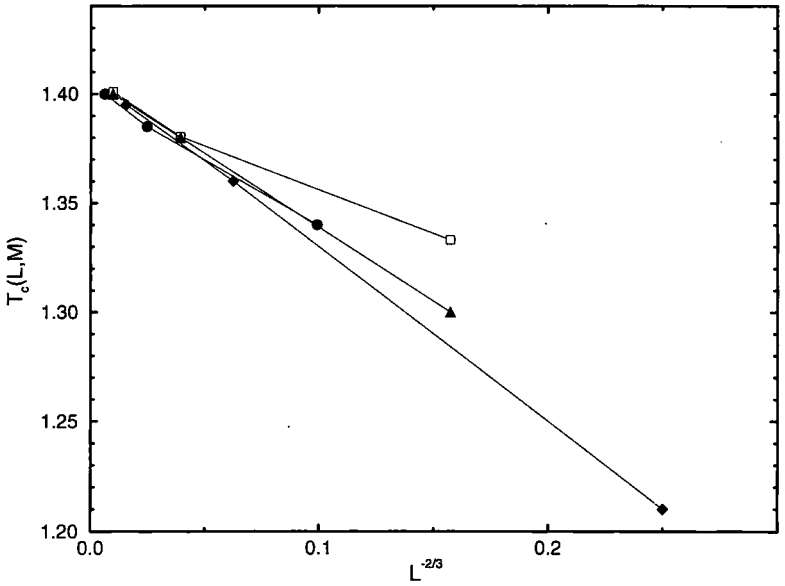

Fig. 2. The locations of the susceptibility peaks plotted against $L^{-2/3}$, for systems with $S = 0.0625$ (diamonds, 8×32, 64×64, and 512×128), $S \approx 0.0787$ (triangles, 16×32, 128×64, and 1024×128), $S \approx 0.157$ (squares, 16×16, 128×32, and 1024×64), and $S \approx 0.198$ (circles, 32×16, 256×32, and 2048×64).

Note that in the scaling region, we would expect that the systems with fixed aspect ratio should approach the same T_c as the system size approaches infinity, independent of the shape of the system. This is clearly not the case when $\nu_\perp = \nu_{||}$ is assumed. Note also that since the system is anisotropic (even if $\nu_\perp = \nu_{||}$, the amplitudes can differ), the square systems do not have special status. The extrapolated T_c values with $\nu_\perp = \nu_{||}/3 = 1/2$ also have nontrivial dependence on S, but the variations are much smaller. Varying $\nu_\perp$ gives qualitatively different curves for T_c vs. S. This indicates that $\nu_\perp = 1/2$ is the correct exponent. Other ratios $\nu_{||}/\nu_\perp = 2$ or 4 do not seem to fit the data well. Thus, Eq. (6) is a good description for the size dependence of the peaks with the set of field-theoretic values. We quote the following value as our final estimate:

$$T_c = 1.408 \pm 0.004 \tag{7}$$

The error given is somewhat objective because of various unknown systematic errors. This result marginally agrees with Leung's result.[8, 9] Some of the previous analyses[7, 10] have been based on square systems and

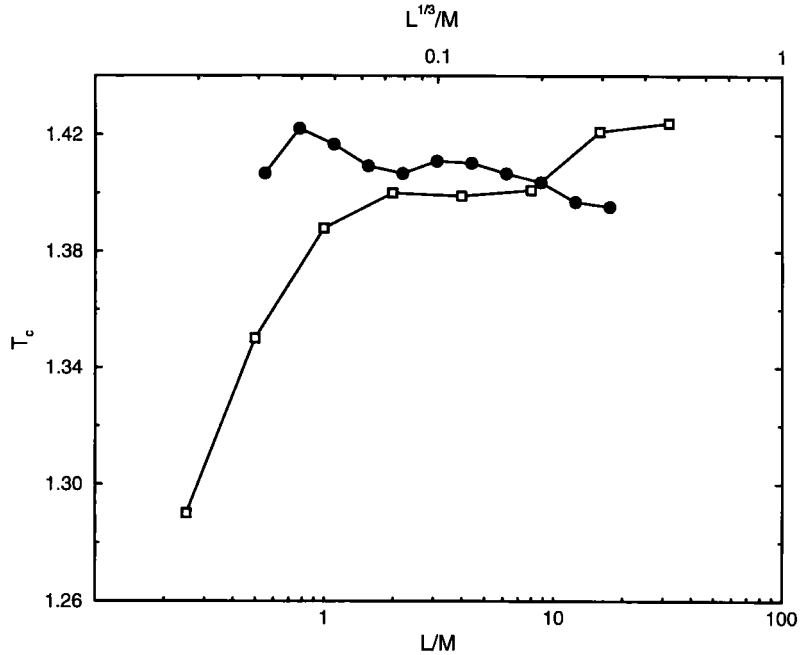

Fig. 3. Extrapolated T_c according to Eq. (6), using the two largest sizes for each S. Circles assume $\nu_\perp = \nu_{||}/3 = 1/2$, upper scale; squares for $\nu_\perp = \nu_{||} = 1$, lower scale.

$\nu_\perp/\nu_{||} \approx 1$. If $\nu_\perp = 1/2$ and $\nu_{||} = 3/2$, the square systems will be more like one-dimensional systems, and perhaps finite-size $T_c(L, L)$ converges very slowly to T_c or not all. This may explain why the previous calculations on square systems all gave a lower T_c. If anisotropy is a dominant feature, we should not expect peak locations to scale simply as $L^{-1/\nu_{||}}$ for square systems.

The peaks were not located with great precision, because the simulations were carried out at discrete points. The second standard method exploits the scaling properties of the fourth-order cumulant. From finite-size scaling theory, we have

$$g(T, L, M) = \tilde{g}(L^{1/\nu_{||}}(T - T_c)/T_c, S) \tag{8}$$

If scaling were exactly obeyed, different curves (with fixed S) should intersect at exactly the same value T_c. Therefore, there is no need to extrapolate to infinite size. In practice there are unknown corrections to scaling. Table II lists the intersection values. The entry at (L, M) is the intersection

Table II. Intersection Value T of the g Functions Between the Systems $L \times M$ and $L/8 \times M/2$

$L\backslash M$	16	32	64	128
32	1.291	1.365	1.380	
64	1.343	1.389	1.400	
128		1.393	1.409	1.414
256		1.392	1.406	1.409
512		1.392	1.403	1.408
1024			1.404	1.415
2048			1.402	

value for T between system $L \times M$ and $L/8 \times M/2$ for the g functions. Table III is similar, but assuming $\nu_\perp = \nu_\parallel$; so it gives the intersection value between system $L \times M$ and $L/2 \times M/2$.

Assuming a fixed S, we see in Table II that the estimated T_c does not depend on L very much. But it slightly increases with M, perhaps due to the influence of the interfaces. If Eq. (8) were exactly obeyed, the intersection temperatures should be independent of L and M. The intersections are consistent with the values from the peak locations. On the other hand, for scaling with fixed aspect ratio, both L and M dependencies are seen. The trend that a larger aspect ratio has a higher intersection value is the same as the peak estimates when $\nu_\parallel = \nu_\perp$ is assumed. This strong size dependence tells us that analysis based on fixed L/M is not appropriate.

We also consider the overall scaling, Eq. (8). The value of T_c for each S can be determined more precisely. However, there are weak size and S dependencies. Nevertheless, we found that the values all fall in the interval 1.395 to 1.410. Figure 4 is one of the scaling plots with $S = 2^{-8/3}$. It is obvious that $T_c = 1.408$ is not the optimal temperature to use for this set

Table III. Intersection Value T of the g Functions Between the Systems $L \times M$ and $L/2 \times M/2$

$L\backslash M$	16	32	64	128	256
16	1.402	1.293	1.256		
32	1.520	1.372	1.332		
64	1.572	1.410	1.371		
128		1.434	1.392	1.379	
256			1.408	1.388	1.38
512			1.414	1.407	
1024			1.414	1.43	
2048			1.409		

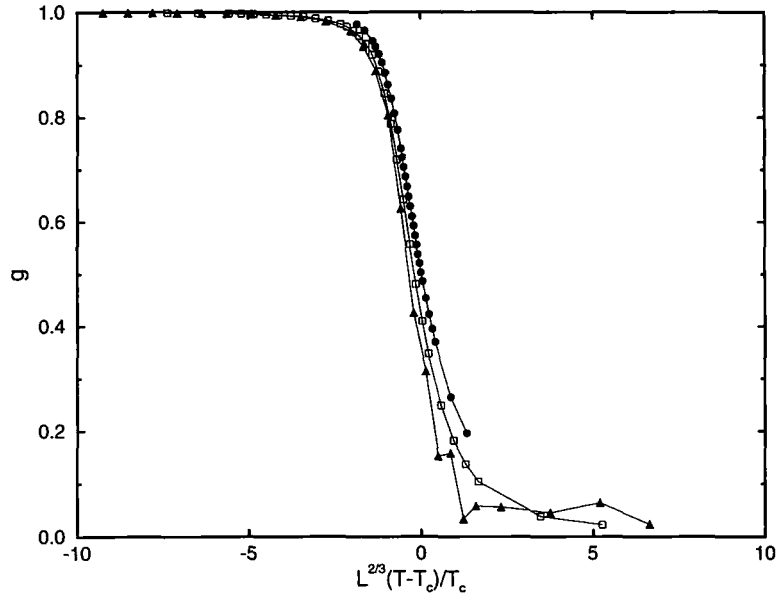

Fig. 4. The fourth-order cumulant g against scaling variable $L^{2/3}(T-T_c)/T_c$; here $T_c = 1.408$. The system sizes are 16×16 (circles), 128×32 (squares), and 1024×64 (triangles).

of data. The value 1.405 will bring a better overlap between the systems $M = 32$ and $M = 64$. Due to corrections to scaling, we cannot find a T so that the three curves coincide. In view of the poor scaling behavior (see also Fig. 8 for the fourth-order cumulant at T_c) and the fact that smaller systems give systematically a lower effective T_c from this sort of analysis, we feel that the estimate $T_c \approx 1.408$ is still consistent with the scaling result of g.

4. ANISOTROPIC FINITE-SIZE SCALING AT THE CRITICAL POINT

In applying the finite-size scaling theory, we could simulate a very large system and study the size effect of smaller subsystems. This may seem computationally effective. But there are two problems associated with it: we have the annoying finite-size effect of the very large system when the subsystem sizes are comparable to it; and we may not be able to equilibrate the very large system very well. So, we adopt the more conventional finite-size scaling analysis—working on fully finite-size rectangles of dimension $L \times M$.

The exponent ratio $\nu_{\|}/\nu_{\perp}$ is one of the most important numbers in an anisotropic finite-size analysis. The theoretical result is often assumed.[8, 18] We have attempted to determine it numerically. The strip geometries with $S \to 0$ or $S \to \infty$ and periodic boundary conditions have simpler scaling behaviours at the critical temperature,[17]

$$\Psi(T_c) \propto M^{\gamma/2\nu_{\perp} - 1/2} L^{-1/2}, \qquad \chi(T_c) \propto M^{\gamma/\nu_{\perp}}, \qquad L \gg M^{\nu_{\|}/\nu_{\perp}} \tag{9}$$

$$\Psi(T_c) \propto L^{\gamma/2\nu_{\|} - 1/2} M^{-1/2}, \qquad \chi(T_c) \propto L^{\gamma/\nu_{\|}}, \qquad M \gg L^{\nu_{\perp}/\nu_{\|}} \tag{10}$$

The value $T_c = 1.41$ is used throughout in this section, since data were computed at this temperature as well as at 1.40 and 1.42. This value appears slightly higher than the actual critical temperature. But the difference between 1.41 and the more precise value 1.408 should be very small. Figure 5 shows the long-strip limiting behaviour for the order parameter. The slopes are $\gamma/(2\nu_{\perp})$ and $\gamma/(2\nu_{\|})$, respectively. The large-L limit is easily achieved, obtaining $\gamma/(2\nu_{\perp}) = 0.96 \pm 0.03$, in accordance with theory. The other limit is hard to reach, because of the slow relaxation in the transverse direction. In any case, we found $\gamma/(2\nu_{\|}) = 0.37 \pm 0.04$. We do not think the crossing of the two straight lines at $L = M = 16$ has any significance. This sort of strip-geometry scaling cannot determine the ratio $\nu_{\|}/\nu_{\perp}$ accurately.

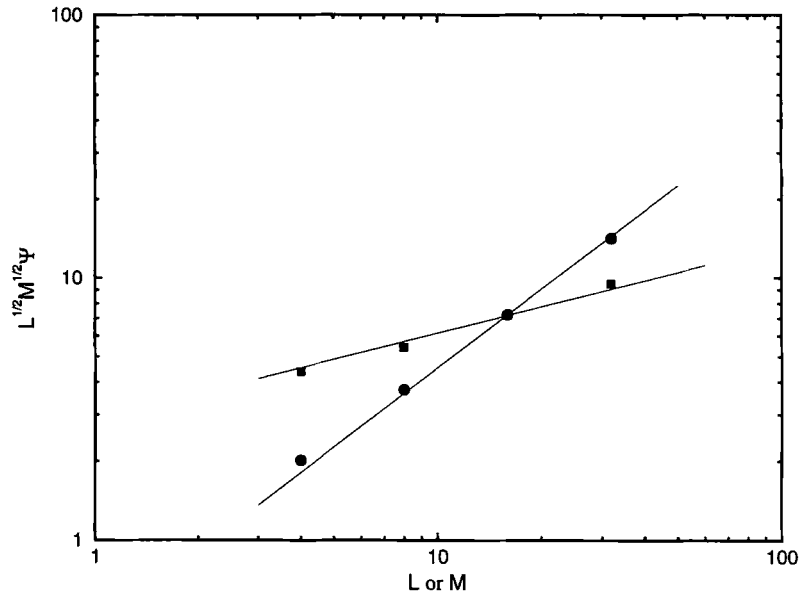

Fig. 5. Order parameter of very long strips at $T_c = 1.41$. Circles are for $L = 1024$ and squares are for $M = 1024$. The straight lines have slopes 1 and 1/3, respectively.

The order parameter or susceptibility at T_c has an extra factor which depends on the ratio S. e.g.,

$$\Psi(T_c, L, M) = M^{-\beta/\nu_\perp} \tilde{\Psi}(L^{\nu_\perp/\nu_\parallel}/M) \tag{11}$$

Moreover, the scaling function obeys $\tilde{\Psi}(S) \to S^{1/2-\beta/\nu_\perp}$ for $S \to 0$ and $\tilde{\Psi}(S) \to S^{-\nu_\parallel/(2\nu_\perp)}$ for $S \to \infty$, as a consequence of the limiting behaviours for very long strips [Eq. (9) and (10)] and the hyperscaling relation

$$2\beta + \gamma = \nu_\perp + \nu_\parallel \tag{12}$$

The scaling form was tested for the Ising model.[17, 19] Previous applications to anisotropic systems were not very successful.[10, 14] Figure 6 is a scaling plot with theoretical values of exponents and $T_c = 1.41$. Similar plots for $T = 1.40$ and 1.42 show definite deviations from scaling. This supports our choice of T_c. The asymptotic slopes for small and large scaling variable S are expected to be $-1/2$ and $-3/2$, respectively. Least-squares fits give -0.50 ± 0.02 and -1.49 ± 0.02 for small and large S, respectively. This

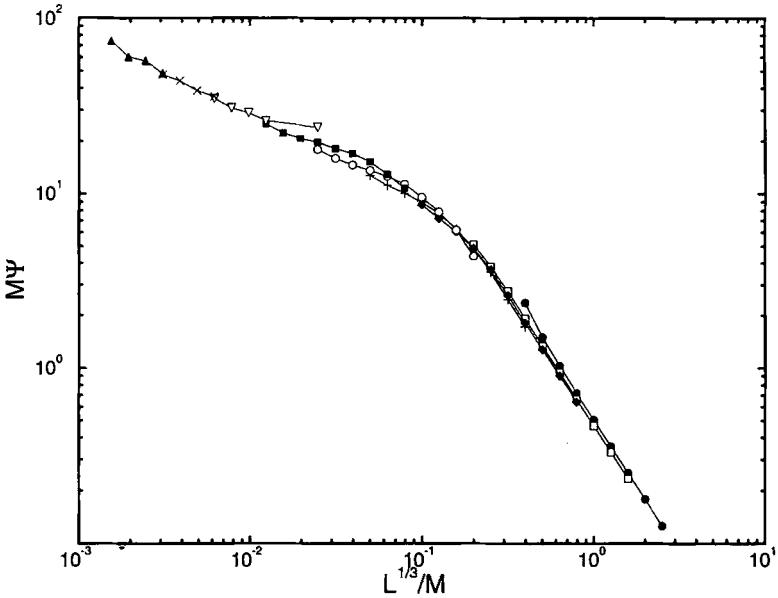

Fig. 6. Scaling plot of the order parameter at the critical point, $T_c = 1.41$. Each set of data has a fixed M value, $M = 4$ (solid circles), $M = 8$ (open squares), $M = 16$ (diamonds), $M = 32$ (pluses), $M = 64$ (open circles), $M = 128$ (squares), $M = 256$ (open triangles), $M = 512$ (crosses), and $M = 1024$ (up triangles).

implies $\beta/\nu_\perp = 1.00 \pm 0.02$ and $\nu_{||}/\nu_\perp = 2.98 \pm 0.04$, in excellent agreement with (1).

Can we obtain good scaling plot if we assume $\nu_{||}/\nu_\perp = 1$ and some choice of $\beta/\nu_\perp$? With the large set of data for various L and M, we can confidently rule out such a possibility.

In Fig. 7 we plot similarly the susceptibility at $T_c = 1.41$ in the scaling form. Plots with $T = 1.40$ and $T = 1.44$ clearly deviate from scaling. The plot with $T = 1.42$ gives roughly the same scaling quality as Fig. 7.

The asymptotic scaling behaviour is borne out,

$$\chi(T_c, L, M) = M^{\gamma/\nu_\perp} \tilde{\chi}(L^{\nu_\perp/\nu_{||}}/M) \tag{13}$$

The scaling function for $S \to 0$ is $\tilde{\chi}(S) \to S^{\gamma/\nu_\perp}$ and for large S, $\tilde{\chi}(S) \to$ const. The data are in full accord with expectations. A least-squares fit to the asymptotic slope gives $\gamma/\nu_\perp = 2.03 \pm 0.03$.

Figure 8 is the scaling plot for the fourth-order cumulant,

$$g(T_c, L, M) = \tilde{g}(L^{\nu_\perp/\nu_{||}}/M) \tag{14}$$

Large finite-size corrections are found here. This is also reflected in the intersection points (Table II). Using data at $T = 1.40$ produces slightly

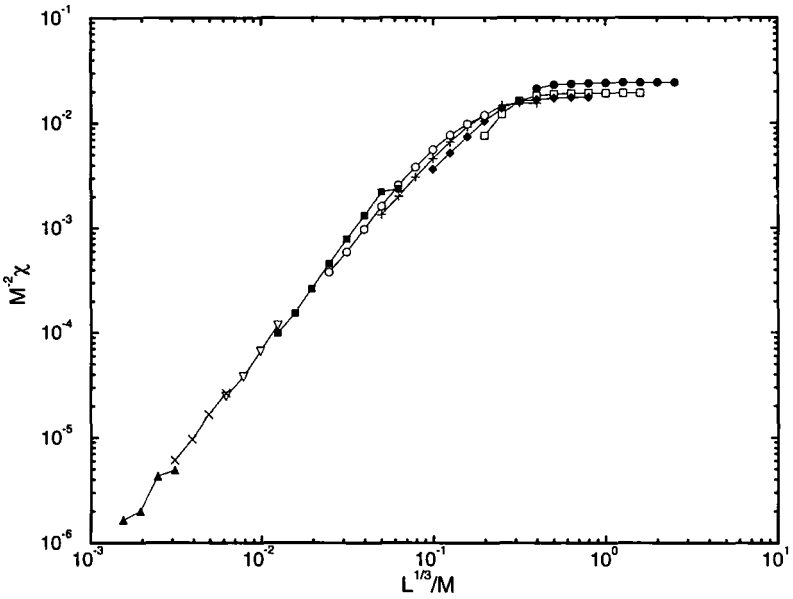

Fig. 7. Scaling plot of the susceptibility at the critical point, $T_c = 1.41$. The symbols are the same as in Fig. 6.

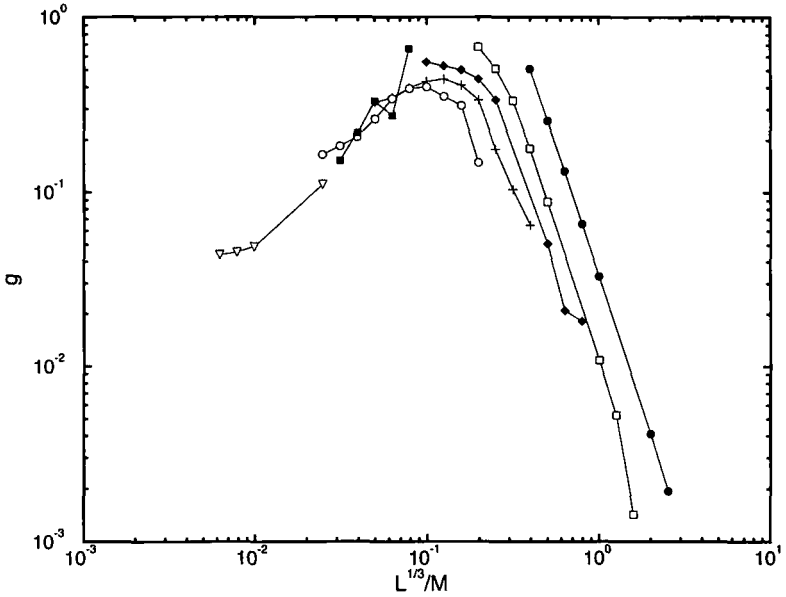

Fig. 8. Scaling plot of the fourth-order cumulant at the critical point. The symbols are the same as in Fig. 6.

better data collapsing. This trend is the opposite of the susceptibility data. In any case, $T = 1.39$ and 1.42 are the temperatures definitely away from T_c. Equation (14) can in principle be used to determine $\nu_\perp/\nu_{||}$. Due to the poor quality of the data, this is not possible for the model.

The higher order moments (χ and g) of the order parameter have larger statistical errors than the order parameter itself. It appears that the corrections to scaling are also large for the higher order moments. Thus, we trust more the scaling of the order parameter. These scaling plots are the first successful application of anisotropic scaling theory to driven diffusive systems. They are good evidence that at least the exponent ratios $\beta/\nu_\perp$, $\gamma/\nu_\perp$, and $\nu_{||}/\nu_\perp$ are in agreement with the field-theoretic values.

5. ANISOTROPIC SCALING AWAY FROM CRITICAL TEMPERATURE

Figure 9 is a plot of the order parameter Ψ for systems with $M = 64$ and $L = 4$–2048. One of the interesting features is that as the system becomes more elongated, it becomes more ordered. This, of course, is consistent with the value of $T_c(L, M)$ in Table I. At low temperatures, because

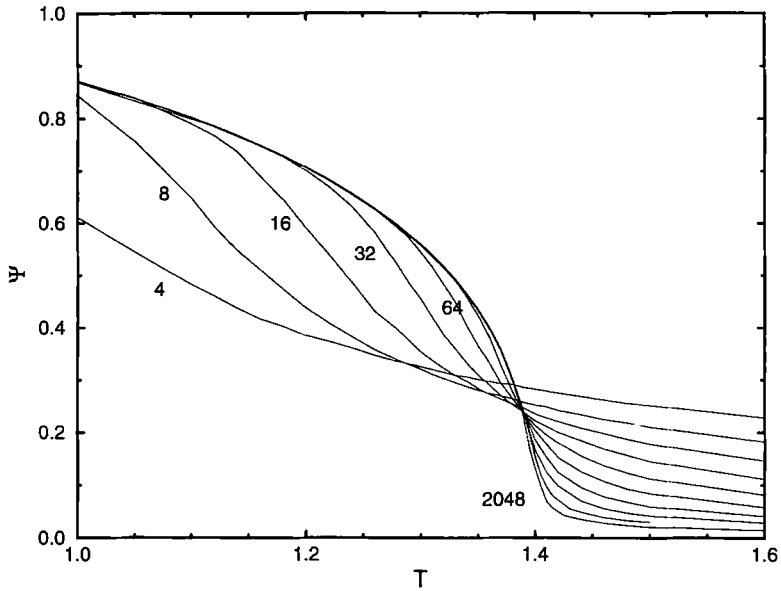

Fig. 9. Order parameter for system size $M = 64$ and various L from 4 to 2048.

of the existence of interfaces, a $1/M$ size dependence is expected, and at higher temperatures we have $\Psi \propto (LM)^{-1/2}$. Near the critical region, we expect

$$\Psi(T, L, M) = L^{\beta/\nu_{||}} \Phi(L^{1/\nu_{||}}(T - T_c)/T_c, S) \tag{15}$$

Leung[8, 9] proposed a stronger scaling form when $S \to 0$. Figure 10 is a scaling plot of the order parameter for $S = 32^{1/3}/16$ with $T_c = 1.408$, assuming the field-theoretic exponents $\beta = 1/2$, $\nu_{\perp} = 1/2$, and $\nu_{||} = 3/2$. The scaling plot is quite sensitive to the choice of T_c and 1.408 is optimal to this set of data. Clear deviations from scaling are seen if 1.404 or 1.411 is used. The $T > T_c$ branch (lower part) obeys scaling very well. The asymptotic slope for large scaling variable is consistent with $-1/2$. For the $T < T_c$ branch (upper part), deviation from scaling is large. We should not simply conclude that the data do not scale for $T < T_c$ since the scaling is valid only for small $|T - T_c|/T_c$ and large L. If we accept that the scaling region for $T < T_c$ is rather narrow, then the scaling plot is not so bad. The asymptotic slope in a properly chosen interval is consistent with $\beta = 1/2$. In any case, the size effect is complicated below T_c. A direct, unambiguous demonstration of the exponent $\beta = 1/2$ is still lacking. It is also not known how much of this can be attributed to possible logarithmic corrections to scaling.

Comparing with Leung's data,[8,9] we feel that his conclusion on data collapse is somewhat too optimistic.

Our order parameter data can be compatible with the exponent $\beta = 1/2$, but only in a rather narrow critical region of $\Delta T = 0.05$ (see Fig. 11). The data can be fitted to a power $\beta \approx 0.3$ in a large temperature region ($\Delta T = 0.3$). This is also roughly the value found in previous work on a square geometry.[7,10] However, if $\beta \approx 0.3$, then we need a critical temperature ($T = 1.385$) which is too low. Fitting the magnetization data to a power law can be unreliable, because the assumption on critical region or T_c has to be made.[16]

The difficulties encountered at low temperatures may be due to uncontrolled finite-size effects or narrow scaling region, or even the use of anisotropic scaling theory, or the set of critical exponents. We also considered the usual isotropic scaling [Eq. (15) with S omitted] using square systems with the critical temperature and exponents in ref. 11. The low-temperature branch scales to some extent. However, the high-temperature branch does not scale at all.

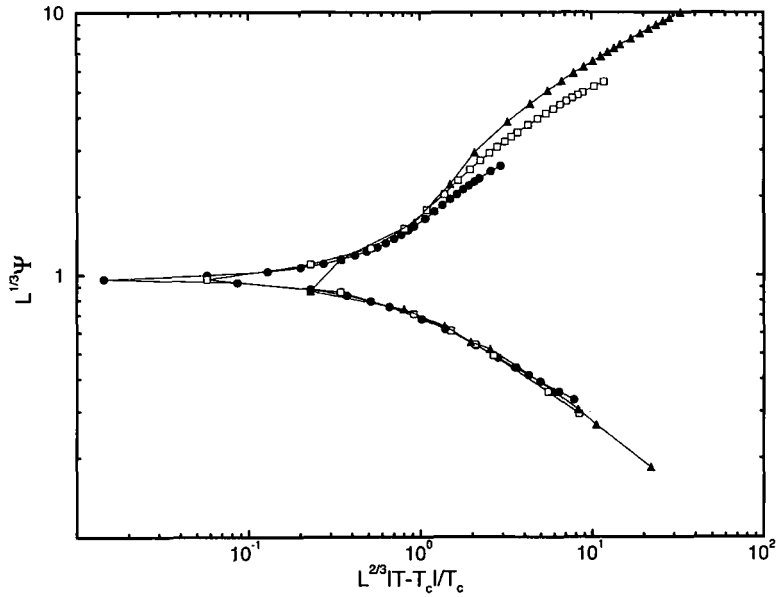

Fig. 10. Scaling plot of the order parameter away from the critical point. The system sizes [Monte Carlo steps] are 32×16 [7×10^8] (circles), 256×32 [1.3×10^8] (open squares), and 2048×64 [4×10^7] (triangles).

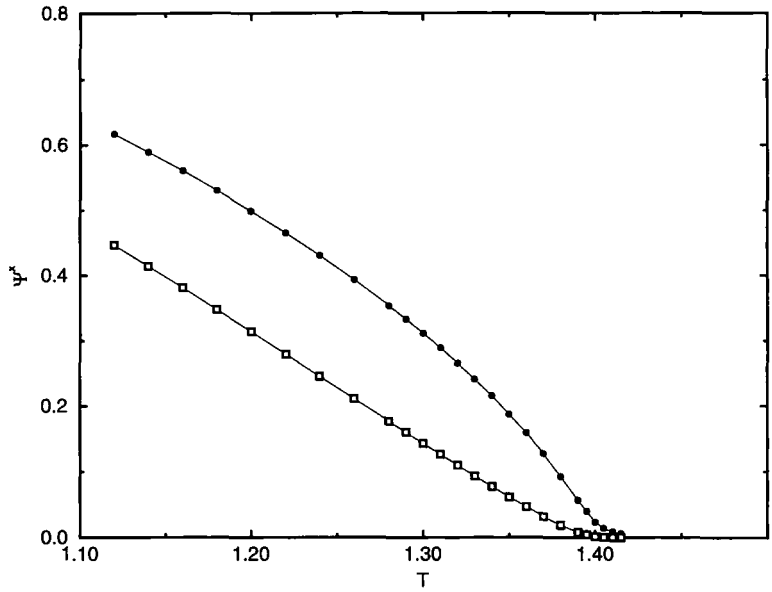

Fig. 11. Order parameter to some power, Ψ^2 (circles) and $\Psi^{10/3}$ (squares), versus temperature T. The system size is 1024×64.

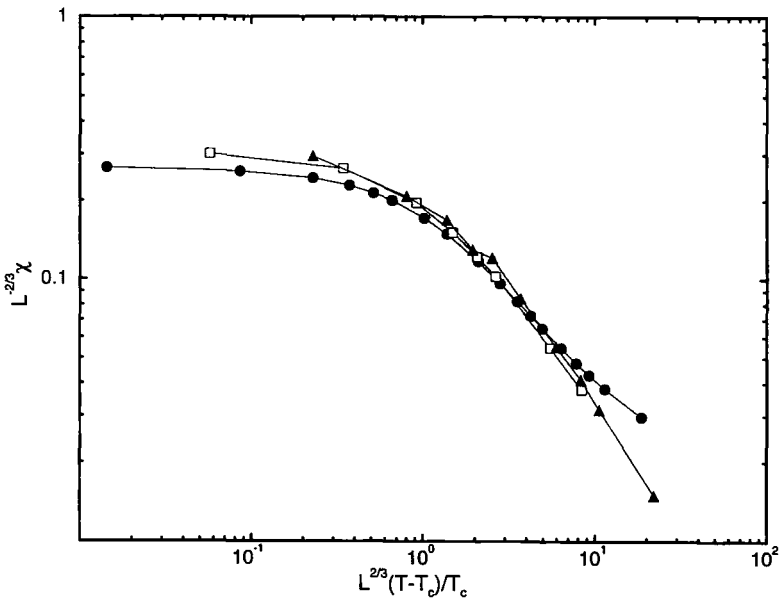

Fig. 12. Scaling plot of the susceptibility χ above the critical temperature. The system sizes are the same as in Fig 10.

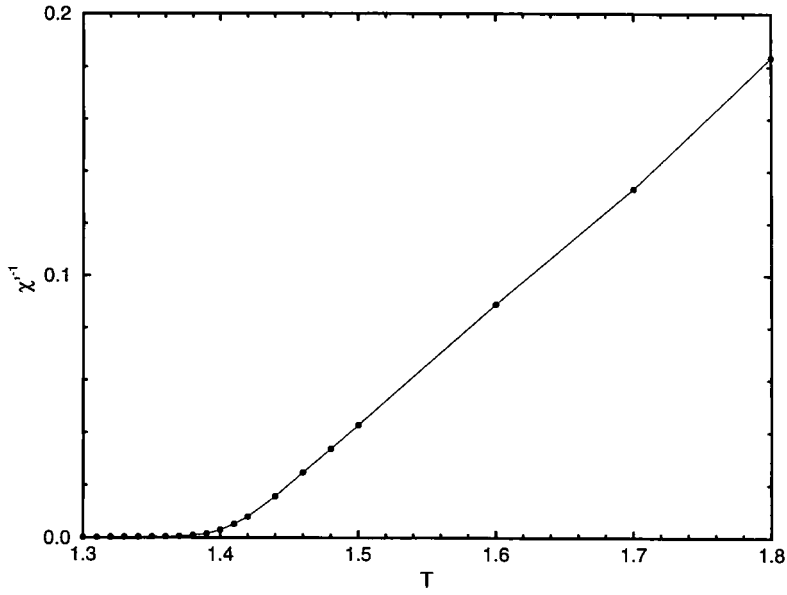

Fig. 13. The inverse susceptibility $(\chi')^{-1}$ against temperature T. The system size is 512×64.

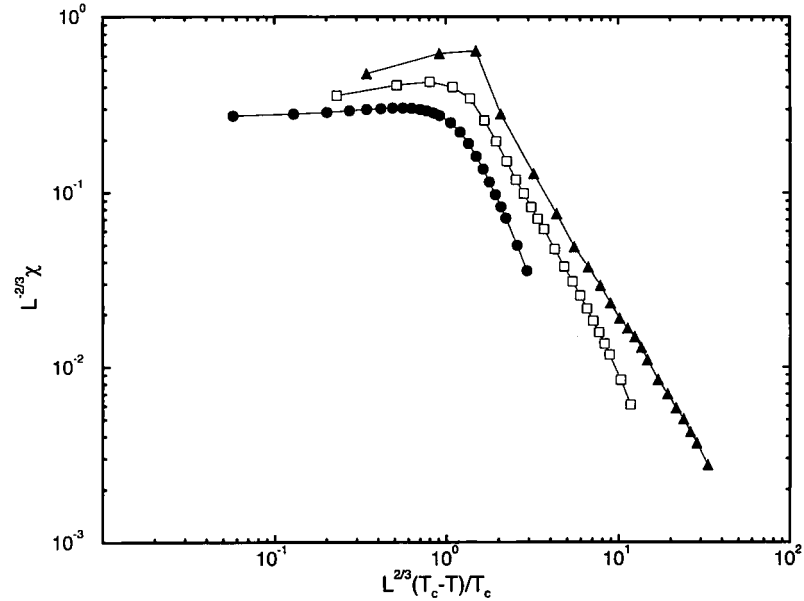

Fig. 14. Scaling plot of the susceptibility χ below the critical temperature. The system sizes are the same as in Fig. 10.

Figure 12 is a scaling plot for the susceptibility χ above the critical temperature. Reasonable data collapse is obtained with the theoretical exponents. The result for χ' is similar, but with somewhat narrower scaling region. The asymptotic slope for large scaling variable $L^{2/3}(T-T_c)/T_c$ is $-\gamma$. Least-squares fits to $\log \chi'$ (or $\log \chi$) vs. $\log(T-T_c)$ for a number of system sizes are consistent with $\gamma = 1$ within a few percent error. The exponent $\gamma = 1$ is also demonstrated by the plot $(\chi')^{-1}$ vs. T in Fig. 13. In such a plot, we expect $(\chi')^{-1} \propto T - T_c$. The value of T_c estimated by linear extrapolation of the curve is in agreement with the results obtained by other methods.

The same set of exponents gives poor scaling for χ below T_c (see Fig. 14). One can bring the data to a better scaling if a larger γ value is used. The fitted exponent γ' strongly depends on M, varying from 1.9 for a 1024×32 system to 1.3 for a 1024×128 system. This behaviour is not well understood.

6. CONCLUSION

Extensive computer simulation of the driven diffusive model has been performed. The data were analyzed by anisotropic finite-size scaling theory. Various forms of corrections to scaling are seen. The order parameter at T_c (Fig. 6) appears to be clean, and has the best scaling property. Away from T_c, the order parameter and susceptibility data below the critical temperature are somewhat difficult to interpret; the question remains open whether the scaling assumption holds below T_c. Nevertheless, the data at and above the critical temperature conform to standard finite-size scaling and are consistent with the phenomenological finite-size scaling theory with the set of exponents derived from the field-theoretic model.

ACKNOWLEDGMENTS

The author thanks Dr. K.-T. Leung and Prof. J. Marro for comments on an earlier version of this paper.

REFERENCES

1. S. Katz, J. L. Lebowitz, and H. Spohn, *Phys. Rev. B* **28**:1655 (1983).
2. S. Katz, J. L. Lebowitz, and H. Spohn, *J. Stat. Phys.* **34**:497 (1984).
3. H. van Beijeren and L S. Schulman, *Phys. Rev. Lett.* **53**:806 (1984).
4. B. Schmittmann, *Int. J. Mod. Phys. B* **4**:2269 (1990); B. Schmittmann and R. K. P. Zia, in *Phase Transitions and Critical Phenomena*, Vol. 17, C. Domb and J. L. Lebowitz, eds. (Academic Press, New York, 1995).
5. H. K. Janssen and B. Schmittmann, *Z. Phys. B* **64**:503 (1986).

6. K.-T. Leung and J. Cardy, *J. Stat. Phys.* **44**:567 (1986).
7. J. L. Vallés and J. Marro, *J. Stat. Phys.* **49**:89 (1987).
8. K.-T. Leung, *Phys. Rev. Lett.* **66**.453 (1991).
9. K.-T. Leung, *Int. J. Mod. Phys. C* **3**:367 (1992).
10. A. Achahbar and J. Marro, *J. Stat. Phys.* **78**:1493 (1995).
11. A. Achahbar, P. L. Garrido, J. Marro, and J. J. Alonso, Preprint (1995); J. Marro, P. L. Garrido, and A. Achahbar, Preprint (1995).
12. H.-O. Heuer, *Computer Phys. Commun.* **59**:387 (1990).
13. N. Kawashima, N. Ito, and Y. Kanada, *Int. J. Mod. Phys. C* **4**:525 (1993).
14. J.-S. Wang, K. Binder, and J. L. Lebowitz, *J. Stat. Phys.* **56**:783 (1989).
15. S. M. Bhattacharjee and J. F. Nagle, *Phys. Rev. A* **31**:3199 (1985).
16. K.-T. Leung and R. K. P. Zia, *J. Stat. Phys.* (in press) (1996).
17. K. Binder and J.-S. Wang, *J. Stat. Phys.* **55**:87 (1989).
18. E. L.-Praestgaard, H. Larsen, and R. K. P. Zia, *Europhys. Lett.* **25**:447 (1994).
19. E. V. Albano, K. Binder, D. W. Heermann, and W. Paul, *Z. Phys. B* **77**:445 (1989).